

Delineating Fluid Reservoirs and the Longevity of Hydrothermal-Gold Events of the Malartic–Val-d’Or Mining Camp in the Southern Abitibi Greenstone Belt, Quebec

M. Herzog¹, C. LaFlamme¹, G. Beaudoin¹ and B. Quesnel¹

¹Département de géologie et de génie géologique, Université Laval, Québec, Québec,

INTRODUCTION

Research in the field of mineral resources will remain pertinent in the future as a means to understanding the associated multiscale processes leading to metal accumulation and their degree of interaction on even smaller scales (i.e., regional-scale tectonics to microscale fluid–rock interactions). The aim of this research project is to decipher the temporal record and footprint of discrete hydrothermal-fluid events at selected orogenic gold deposits of the strongly gold-endowed and geochemically well-studied area of the Malartic–Val-d’Or mining camp of the Abitibi Subprovince (Beaudoin and Pitre, 2005; Beaudoin and Chiaradia, 2016). Pulling apart and understanding the lithological and structural relationships of individual hydrothermal-fluid events will be completed at the camp scale by combining regional-scale field observations taken along the Malartic transects, with detailed and temporally constrained observations made at distinct orogenic gold deposits and showings at the mineral grain scale. Sulphur forms the most important complexing ligand for the precipitation of gold-bearing sulphide minerals from aqueous fluids (e.g., Loucks and Mavrogenes, 1999); therefore, tracing its pathways is essential in determining exactly what reservoirs, structures and processes lead to the accumulation of gold at the camp-scale (e.g., Farquhar and Wing, 2003; LaFlamme et al., 2018).

Preliminary field observations indicate that subeconomic gold deposition in the volcanic sequences in the Malartic–Val-d’Or area may have contributed to the exceptional endowment in gold recorded in the structurally controlled, late-stage quartz-tourmaline±carbonate shear veins of the Abitibi Subprovince. Subsequent results of this project will inform on the longevity of single- or multiphased hydrothermal-gold events, as well as on the source and various physicochemical conditions leading to gold precipitation at the camp scale. The knowledge required for the successful exploration of orogenic gold deposits will also benefit from the simple application of in situ high-resolution analytical techniques such as U-Pb geochronology using laser-ablation inductively coupled plasma–mass spectrometry (LA-ICP-MS), multiple sulphur isotope analyses by secondary-ion mass spectrometry (SIMS), triple quadrupole LA-ICP-MS and Re-Os isotope analyses, as well as quantitative mapping by LA-ICP-MS at the sulphide-mineral scale. Moreover, it will contribute to a deeper understanding of the link between gold and sulphur endowment in economically viable nascent and barren target regions, and the related Archean ore-forming processes.

REGIONAL GEOLOGY

The Abitibi Subprovince, an Archean greenstone terrane located at the southeastern margin of the Superior craton, consists of low- to moderate-grade metamorphic rocks (Figure 1) that display well-preserved primary geological relationships recorded in metamorphosed intrusive and volcanic rocks, as well as metamorphosed sedimentary rocks. Major ultramafic, mafic and felsic submarine volcanic successions (ca. 2795–2695 Ma) and temporally associated tonalitic, granodioritic, dioritic and monzonitic domes of intrusive rocks record a predominant steeply dipping, east-striking foliation that developed during burial and major crustal thickening. Thick-skinned tectonics bracketed between ca. 2690 and 2669 Ma caused the onset of unconformably overlying flysch- and molasse-like sedimentary rocks derived from terrestrial environments (e.g., Pyke et al.,

1973; Dimroth et al., 1978; Hyde, 1980; Ross et al., 2011a, b; Monecke et al., 2017). Major precious- and base-metal deposits are accumulated at the southern contact with the high-grade metamorphic sedimentary rocks of the Pontiac Subprovince, which is defined through the east–west-striking, long-lived Larder Lake–Cadillac fault zone (LLCFZ) and north-branching Porcupine–Destor fault zone (PDFZ; e.g., Ayer et al., 2005; Thurston et al., 2008; Hastie et al., 2016, Bedeaux et al., 2017). Gold mining camps spatially associated along these two structural corridors contain up to 6043.4 t (194.3 million ounces) of gold, with 2765.1 t (88.9 million ounces) in the PDFZ camps and up to 3278.3 t (105.4 million ounces) in the LLCFZ camps; 27.3% of the total, or 1649.7 t (53.04 million ounces), lie in the Malartic–Val-d’Or mining camp (Gosselin and Dubé, 2005; Dubé and Gosselin, 2007; Dubé et al., 2017; Monecke et al., 2017).

METHODOLOGY

The framework for this study is built upon structurally controlled samples from various orogenic gold deposits and occurrences throughout the Malartic–Val-d’Or mining camp, with fieldwork completed in 2019 at the Canadian Malartic, Goldex, Triangle and Pascalis Gold Trend deposits. Structural, lithological and alteration relationships between veins, mineralization and host-rock lithologies were logged and verified to be temporally and spatially constrained at the camp scale. Representative samples will undergo optical petrography, detailed sulphide-mineral assemblage characterization and determination of a petrogenetic sequence by scanning electron microscopy to establish both the timing of mineralization in the sequences and the relationship between sulphide minerals and gold. In situ LA-ICP-MS analysis of the radiogenic accessory mineral xenotime will be used to date those previously characterized distinct hydrothermal-fluid events and sulphide mineral assemblages (e.g., Petrella et al., 2019). In addition, analysis of multiple sulphur isotopes using SIMS (LaFlamme et al., 2016) will reveal the different sulphur reservoirs responsible for ore deposit genesis and changing P-T-oxygen fugacity conditions at the mineral-grain scale. Moreover, a new approach to multiple sulphur isotope analysis by triple quadrupole LA-ICP-MS will be attempted to decrease sample preparation and analysis time (e.g., Diez Fernández et al., 2012). Additional quantitative mapping by LA-ICP-MS of individual sulphide mineral assemblages will aid in characterizing distinct geochemical footprints of hydrothermal-gold events at the mineral-grain scale. Ultimately, paragenetically well-characterized sulphide mineral assemblages will be analyzed for their corresponding Re-Os isotope concentrations to identify any involvement of potential crustal components in the fluid reservoirs, as shown by Mathur et al. (2000) or Ootes et al. (2011).

MALARTIC–VAL-D’OR MINING CAMP GEOLOGY AND MINERALIZATION

In the Malartic–Val-d’Or mining camp, the predominant chronostratigraphic assemblages comprise the volcanic sequences of the Kidd–Munro (2720–2710 Ma), Tisdale (2710–2704 Ma) and Blake River (2704–2695 Ma) assemblages, as well as the sedimentary sequences of the Porcupine (2690–2685 Ma) and Timiskaming (2679–2669 Ma) assemblages (Ayer et al., 2002, 2005; Thurston et al., 2008; Monecke et al., 2017). Most gold mineralization between the townships of Malartic and Val-d’Or occurs in the Tisdale and Blake River assemblages (Figure 1), which straddle the east-southeast-trending LLCFZ that juxtaposes high-grade metamorphic rocks of the Pontiac Subprovince to the south. The volcanogenic and metallogenic evolution of the Malartic–Val-d’Or camp is reflected in the more detailed nomenclatures of Pilote et al. (1997) and Scott et al. (2002), which build on the early works of Latulippe (1966), Imreh (1984) and Dimroth et al. (1983a), who coined the widely used term ‘Malartic Group’ and its lithological units. The lowermost lithological unit of the Malartic group, the La Motte–Vassan formation (2714 ± 2 Ma), contains komatiites and other effusive ultramafic rocks. Subsequently, the Dubuisson formation (2708 ± 2 Ma) records continued magmatic evolution and comprises ultramafic to mafic volcanic rocks, with local felsic rocks (Pilote et al., 1997, 1998a, b, c). The topmost lithological member of the Malartic group, the Jacola formation (2706 ± 2 Ma), predominantly consists of mafic volcanic rocks and hyaloclastites, recording the interaction with Archean seawater and indicating emplacement at shallow levels (Machado and Gariépy, 1994). Conformably overlying the Malartic group, the Louvicourt group consists of the Val d’Or formation (2704 ± 1 Ma), with basaltic pillow lavas and pyroclastic andesitic rocks, and

the Héva Formation (2702 ±2 Ma), with mafic to felsic volcanoclastic rocks (Machado and Gariépy, 1994; Pilote et al., 1998a, b, c).

An early compressive deformation phase (D₁) caused folding and tilting of the volcanic sequence and an overall dip to the north. Gold-hosting structures in the southern Abitibi Subprovince are intimately related with the subsequent compressive deformation phase (D₂), which led to the formation of a predominant east–west- to northwest-striking, almost subvertical S₂ fabric, proximal to several east–west-trending structural segments that merge to form the LLCFZ (Bedeaux et al., 2017). This regional fabric is crosscut by second and third order low- to high-angle reverse shear zones related to D₃, a late-stage dextral strike-slip movement along the LLCFZ, which host the majority of mineralized orogenic gold veins (Robert et al., 2005; Dubé and Gosselin, 2007; Dubé et al., 2017). Orogenic gold veins in the Malartic–Val-d’Or camp commonly display quartz-carbonate or quartz-tourmaline-carbonate vein mineral assemblages, with variable sulphide contents observed either in altered hostrock envelopes with veins or in sulphide mineral agglomerates within the veins (e.g., Robert et al., 2005). Simultaneously, low- to medium-grade regional metamorphism affects the Abitibi Subprovince and is inferred between 2669 and 2643 Ma (Powell et al., 1995). A suite of syntectonic alkaline intrusions (2685–2671 Ma) and metamorphosed rocks of the Pontiac Subprovince hosts the Canadian Malartic disseminated-stockwork gold deposit (2664 ±11 Ma; De Souza et al., 2017). Numerous intrusive rocks hosting gold mineralization are found to the east; for example, the south-dipping quartz-tourmaline veins of the Goldex deposit (Figure 1) are hosted in a bedding-parallel granodiorite sill and the south-dipping quartz-tourmaline±carbonate veins of the Triangle deposit, along shear zones within a subvertical diorite intrusion. At the Pascalis Gold Trend deposit, to the west of the pre-2695 Ma tonalitic to granodioritic Bourlamaque batholith (Wong et al., 1991), gold mineralization is spatially associated with stacked sets of subhorizontal quartz-tourmaline veins.

PRELIMINARY RESULTS

Based on crosscutting relationships observed during this field season, a set of preliminary vein parageneses at selected structurally controlled gold deposits throughout the Malartic–Val-d’Or mining camp (Figure 2) records heterogeneous vein mineral assemblages. All the veins crosscut the pervasive east- to northwest-trending, subvertical S₂ foliation developed in the (meta-) volcanic, intrusive and sedimentary hostrock sequence. At the Canadian Malartic deposit, four generations of veins in the Barnat and Sladen orebodies of the planned East Malartic extension, located in the LLCFZ, are hosted in silicified, strongly albitized porphyritic diorite, and silicified and weaker albitized argillite/greywacke, respectively. Bluish and undulatory, centimetre-sized second-generation veins at the Canadian Malartic deposit (V_{2CM}; quartz–albite–K-feldspar±biotite±sulphides) trend into massive, clear quartz veins of up to 1 m in thickness and host minor gold. The partly brecciated, centimetre-sized V_{3CM} veins host most of the millimetre-sized pyrite and associated gold mineralization in a quartz-ankerite-calcite-albite-biotite/chlorite-sulphide±epidote±hematite vein assemblage. In contrast, the four generations of veins identified at the Goldex deposit mineralized, fracture-infilled quartz-tourmaline vein assemblage, which was formed in a single shear zone, display strong albite-sericite and tourmaline alteration related to vein formation in the granodiorite host. An early set of flat, low-grade V_{1GX} veins of fluorite-tourmaline-chlorite±epidote contains <2% pyrite. As they approach 0.5 to 1 m wide shear zones, the flat V_{1GX} trend into major gold-bearing shear zones comprising quartz-tourmaline-pyrite-fluorite-carbonate-chlorite±epidote and millimetre- to centimetre-sized pyrite and sulphide (contents between 10–15%), predominantly related to tourmalinized vein areas.

Quartz-tourmaline veins of the Triangle deposit, at the Lamaque property, share similarities with the mineralized veins at the Goldex deposit, such as a pervasive quartz-sericite-albite alteration of the subvertical diorite and silicified basaltic–andesitic volcanic hostrocks. Nevertheless, anastomosing, high-angle reverse shear zones host at least four different generations of veins that pinch and swell along the same structure, consisting of massive quartz-tourmaline that reaches a thickness of up to 7 m in some parts of the veins. A subset of quartz-tourmaline±carbonate V_{2LQ} veins documents a precursor to mineralization, with low gold grades and locally

traces (<2%) of sulphide minerals. The V2ALQ subset hosts gold in millimetre- to centimetre-sized pyrite grains, primarily observed in a tourmaline breccia±quartz. Most gold occurs in the centre of the reverse shear zones in the form of V3LQ quartz-carbonate-sulphide veins (sulphide content of 15–20%) hosting visible gold in pyrite-chalcopyrite-sulphide aggregates several centimetres in size, with local traces of honeycomb sphalerite and brown galena. At the newly developed Pascalis Gold Trend deposit, quartz-tourmaline veins up to 1.5 m thick occur along subvertical sinistral shear zones, with stacked subhorizontal centimetre- to metre-sized flat veins dissecting mafic intrusive and mafic volcanic hostrocks, and also form between the shear zones. Four contrasting generations of veins host mineralization occurring for the most part in thin, early sulphide-rich veins or an alteration envelope, which is developed in a variety of hostrocks, surrounding the later veins. The most observed alteration processes related to quartz-tourmaline vein infill are replacement by chlorite and quartz, and tourmalinization. A first set of low to intermediate gold-grade veins (V0PGT and V1PGT) observed in a basalt (Figure 3) occurs subparallel to S₀ and consists of thin, millimetre- to centimetre-sized sulphide-quartz±carbonate and quartz-sulphide vein assemblages. Nevertheless, a second set of dolomite-quartz veins (V2PGT) and quartz-tourmaline±carbonate veins (V3PGT) hosts most gold either at the contact of the vein with the hostrock or in tourmalinized alteration halos in euhedral pyrite grains of up to 5 cm in size. Preliminary field observations indicate that low gold contents of <0.5 ppm already could have been present in the volcanic hostrock sequence prior to the main compressive D₂ and D₃ deformation events that led to the formation of most gold-endowed second- and third-order structures in the Malartic–Val-d’Or camp.

ACKNOWLEDGMENTS

This Ph.D. study project is funded by Metal Earth, through the Canada First Research Excellence Fund. The authors wish to express their gratitude to all the employees at Agnico Eagle, Canadian Malartic, Eldorado Gold and Probe Metals Inc. who provided their aid in the organizational aspects of the project and granted access to the mine sites and core shacks. The help of the Metal Earth project staff and Malartic transect staff, as well as the undergraduate field assistant I. Stephenson, were especially appreciated.

This project is part of a Ph.D. thesis project by Michael Herzog in the Département de géologie et de génie géologique at the Université Laval under the supervision of Dr. Crystal LaFlamme and Dr. Georges Beaudoin.

Harquail School of Earth Sciences, Mineral Exploration Research Centre contribution MERC-ME-2019-235.

REFERENCES

- Ayer, J.A., Amelin, Y., Corfu, F., Kamo, S., Ketchum, J., Kwok, K. and Trowell, N. 2002. Evolution of the southern Abitibi greenstone belt based on U-Pb geochronology: autochthonous volcanic construction followed by plutonism, regional deformation and sedimentation; *Precambrian Research*, v. 115, p. 63–95.
- Ayer, J.A., Thurston, P.C., Bateman, R. Dubé, B., Gibson, H.L., Hamilton, M.A., Hathway, B., Hocker, S.M., Houlié, M.G., Hudak, G., Ispolatov, V.O., Lafrance, B., Leshner, C.M., MacDonald, P.J., Péloquin, A.S., Piercey, S.J., Reed, L.E. and Thompson, P.H. 2005. Overview of results from the Greenstone Architecture Project: Discover Abitibi Initiative; Ontario Geological Survey Open File Report 6154, 146 p.
- Beakhouse, G.P. 2011. The Abitibi subprovince plutonic record: tectonic and metallogenic implications; Ontario Geological Survey Open File Report 6268, 161 p.
- Beaudoin, G. and Pitre, D. 2005. Stable isotope geochemistry of the Archean Val-d’Or (Canada) orogenic gold vein field; *Mineralium Deposita*, v. 40, p. 59–75.

- Beaudoin, G. and Chiaradia, M. 2016. Fluid mixing in orogenic gold deposits: evidence from the H-O-Sr isotope composition of the Val-d'Or vein field (Abitibi, Canada); *Chemical Geology*, v. 437, p. 7–18.
- Bedeaux, P., Pilote, P., Daigneault, R. and Rafini, S. 2017. Synthesis of the structural evolution and associated gold mineralization of the Cadillac fault, Abitibi, Canada; *Ore Geology Reviews*, v. 82, p. 49–69.
- Couture, J.-F., Pilote, P., Machado, N. and Desrochers, J.-P. 1994. Timing of gold mineralization in the Val-d'Or district, southern Abitibi belt: evidence for two distinct mineralizing vents; *Economic Geology*, v. 89, p. 1542–1551.
- Davis, W.J., Machado, N., Gariépy, C., Sawyer, E.W. and Benn, K. 1994. U-Pb geochronology of the Opatika tonalite-gneiss belt and its relationship to the Abitibi greenstone belt, Superior province, Quebec; *Canadian Journal of Earth Sciences*, v. 32, p. 113–127.
- De Souza, S., Dubé, B., McNicoll, V.J., Dupuis, C., Mercier-Langevin, P., Creaser, R.A. and Kjarsgaard, I.M. 2017. Geology and hydrothermal alteration of the world-class Canadian Malartic gold deposit: genesis of an Archean stockwork-disseminated gold deposit in the Abitibi Greenstone Belt, Québec; *Reviews in Economic Geology*, v. 19, p. 263–291.
- Diez Fernández, S., Sugishama, N., Ruiz Encinar, J. and Sanz-Medel, A. 2012. Triple quad ICP-MS (ICPQQQ) as a new tool for absolute quantitative proteomics and phosphoproteomics; *Analytical Chemistry*, v. 84, p. 5851–5857.
- Dimroth, E., Cousineau, P., Leduc, M. and Sanschagrin, Y. 1978. Structure and organization of Archean subaqueous basalt flows, Rouyn-Noranda area, Quebec, Canada; *Canadian Journal of Earth Sciences*, v. 15, p. 902–918.
- Dimroth, E., Imreh, L., Goulet, N. and Rocheleau, M. 1983. Evolution of the south-central segment of the Archean Abitibi belt, Quebec, Part II: tectonic evolution and geomechanical model; *Canadian Journal of Earth Sciences*, v. 20, p. 1355–1373.
- Dubé, B., Gosselin, P., Mercier-Langevin, P., Hannington, M. and Galley, A. 2007. Gold-rich volcanogenic massive sulphide deposits; *in* Mineral deposits of Canada: a synthesis of major deposit-types, district metallogeny, the evolution of geological provinces, and exploration methods, (ed.) W.D. Goodfellow; Geological Association of Canada, Mineral Deposits Division, Special Publication no. 5, p. 75–94.
- Dubé, B., Mercier-Langevin, P., Ayer, J., Atkinson, B. and Monecke, T. 2017. Orogenic greenstone-hosted quartz-carbonate gold deposits of the Timmins-Porcupine camp; *Reviews in Economic Geology*, v. 19, p. 51–79.
- Farquhar, J. and Wing, B. 2003. Multiple sulfur isotopes and the evolution of the atmosphere; *Earth and Planetary Science Letters*, v. 213, p. 1–13.
- Gosselin, P. and Dubé, B. 2005. Gold deposits of the world: distribution, geological parameters and gold content; Geological Survey of Canada, Open File 4895, 271 p.
- Hastie, E.C.G., Kontak, D.J. and Lafrance, B. 2016. Update on activities related to a gold metallogenic study of the southern Swayze greenstone belt; *in* Summary of Field Work and Other Activities, 2016; Ontario Geological Survey, Open File Report 6323, p. 8-1–8-10.
- Hyde, R.S. 1980. Sedimentary facies in the Archean Timiskaming Group and their tectonic implications, Abitibi greenstone belt, northeastern Ontario, Canada; *Precambrian Research*, v. 12, p. 161–195.

- Imreh, L. 1984. Sillon de La Motte–Vassan et son avant-pays méridional: synthèse volcanologique, lithostratigraphique et gîtologique; Ministère de l'Énergie et des Ressources du Québec, report MM 82-04, 72 p.
- Jemielita, R.A., Davis, D.W. and Krogh, T.E. 1990. U-Pb evidence for Abitibi gold mineralization postdating greenstone magmatism and metamorphism; *Nature*, v. 346, p. 831–834.
- LaFlamme, C., Martin, L., Jeon, H., Reddy, S.M., Selvaraja, V., Caruso, S., Bui, T.H., Roberts, M.P., Voute, F., Hagemann, S., Wacey, D., Littman, S., Wing, B., Fiorentini, M. and Kilburn, M.R. 2016. In situ sulfur isotope analysis by SIMS of pyrite, chalcopyrite, pyrrhotite, and pentlandite to refine magmatic ore genetic models; *Chemical Geology*, v. 444, p. 1–15.
- LaFlamme, C., Fiorentini, M.L., Lindsay, M.D. and Bui, T.H. 2018. Atmospheric sulfur is recycled to the crystalline continental crust during supercontinent formation; *Nature Communications*, v. 9, p. 1–9.
- Latulippe, M. 1966. The relationship of mineralization to Precambrian stratigraphy in the Matagami Lake and Val-d'Or districts of Québec; *Geological Association of Canada*, v. 3, p. 21–42.
- Loucks, R.R. and Mavrogenes, J.A. 1999. Gold solubility in supercritical hydrothermal brines measured in synthetic fluid inclusions; *Science*, v. 284, p. 2159–2163.
- Machado, N., Philippe, S., Gariépy, C. and David, J. 1991. Géochronologie U-Pb territoire québécois: fosses du Labrador et de l'Ungava et Sous-province du Pontiac; Ministère de l'Énergie et des Ressources du Québec, MB 91-07, 50 p.
- Machado, N. and Gariépy, C. 1994. Géochronologie U-Pb du territoire québécois : la Sous-province de l'Abitibi, cinquième rapport intérimaire : résultats 1993–1994; Ministère des Ressources naturelles du Québec, internal report, 9 p.
- Mathur, R., Ruiz, J., Titley, S., Gibbins, S. and Margotomo, W. 2000. Different crustal sources for the Au-rich and Au-poor ores of the Grasberg Cu-Au porphyry deposit; *Earth and Planetary Science Letters*, v. 183, p. 7–14.
- Monecke, T., Mercier-Langevin, P., Dubé, B. and Friedman, B.M. 2017. Geology of the Abitibi greenstone belt; Chapter 1 *in* Archean base and precious metal deposits, (ed.) T. Monecke, P. Mercier-Langevin and B. Dubé; *Reviews in Economic Geology*, v. 19, p. 7–50.
- Morasse, S., Wasteneys, H.A., Cormier, M., Helmstaedt, H. and Mason, R. 1995. A pre-2686 Ma intrusion-related gold deposit at the Kiena mine, Val d'Or, Québec, Southern Abitibi Subprovince; *Economic Geology*, v. 90, p. 1310–1321.
- Ootes, L., Morelli, R.M., Creaser, R.A., Lentz, D.R., Falck, H. and Davis, W.J. 2011. The timing of Yellowknife gold mineralization: a temporal relationship with crustal anataxis?; *Economic Geology*, v. 106, p. 713–720.
- Petrella, L., Thébaud, N., LaFlamme, C., Miller, J., McFarlane, C., Occhipinti, S., Turner, S. and Perazzo, S. 2019. Contemporaneous formation of vein-hosted and stratabound gold mineralization at the world-class Dead Bullock Soak mining camp, Australia; *Mineralium Deposita*, 18 p..
- Piette-Lauzière, N., Guilmette, C., Bouvier, A., Perrouty, S., Pilote, P., Gaillard, N., Lypaczewski, P., Linnen, R.L. and Olivo, G.R. 2019. The timing of prograde metamorphism in the Pontiac Subprovince, Superior craton: implications for Archean geodynamics and gold mineralization; *Precambrian Research*, v. 320, p. 111–136.

- Pilote, P., Dion, C., Joannis, A., David, J., Machado, N., Kirkham, R.V. and Robert, F. 1997. Géochronologie des minéralisations d'affiliation magmatique de l'Abitibi, secteurs Chibougamau et de Troilus-Frotet : implications géotectoniques; Programme et résumés, Séminaire d'information sur la recherche géologique ; Ministère des Ressources naturelles, Québec, DV97-03, 47 p.
- Pilote, P., Moorhead, J. and Mueller, W. 1998a. Développement d'un arc volcanique, la région de Val-d'Or, ceinture de l'Abitibi—volcanologie physique et évolution métallogénique; Geological Association of Canada—Mineralogical Association of Canada, Joint Annual Meeting, Québec, Québec, May 1998, Fieldtrip guidebook A2, 104 p.
- Pilote, P., Mueller, W.U., Parent, M., Machado, N., Moorhead, J., Scott, C.R. and Lavoie, S. 1998b. Géologie et volcanologie des formations Val-d'Or et Héva, district de Val-d'Or, sous-province de l'Abitibi Québec: contraintes géochimique et géochronologique; Geological Association of Canada—Mineralogical Association of Canada, Joint Annual Meeting, Québec, Québec, May 1998,, Program with Abstracts, p. 146–47.
- Pilote, P., Mueller, W., Scott, C., Lavoie, S., Champagne, C. and Moorhead, J. 1998c. Volcanologie de la formation de Val-d'Or et du groupe de Malartic, Sous-province de l'Abitibi: contraintes géochimiques et géochronologiques; Ministère des Ressources naturelles du Québec, DV 98-05, 48 p.
- Powell, W.G., Carmichael, D.M. and Hodgson, C.J. 1995. Conditions and timing of metamorphism in the southern Abitibi greenstone belt, Quebec; Canadian Journal of Earth Sciences, v. 32, p. 787–805.
- Pyke, D.R., Naldrett, A.J. and Eckstrand, O.R. 1973. Archean ultramafic flows in Munro Township, Ontario; Geological Society of America, Bulletin 84, p. 955–978.
- Robert, F., Poulsen, K.H., Cassidy, K.F. and Hodgson, C.J. 2005. Gold metallogeny of the Superior and Yilgarn cratons; *in* Economic Geology One Hundredth Anniversary Volume, (ed.) J.W. Hedenquist, J.F.H. Thompson, R.J. Goldfarb and J.P. Richards; Society of Economic Geologists, , p. 1001–1033.
- Ross, P.S., Goutier, J., Mercier-Langevin, P. and Dubé, B. 2011a. Basaltic to andesitic volcanoclastic rocks in the Blake River Group, Abitibi greenstone belt: 1. Mode of emplacement in three areas; Canadian Journal of Earth Sciences, v. 48, p. 728–756.
- Ross, P.S., McNicoll, V., Goutier, J., Mercier-Langevin, P. and Dubé, B. 2011b. Basaltic to andesitic volcanoclastic rocks in the Blake River Group, Abitibi greenstone belt: 2. Origin, geochemistry and geochronology; Canadian Journal of Earth Sciences, v. 48, p. 757–777.
- Scott, C.R., Mueller, W.U. and Pilote, P. 2002. Physical volcanology, stratigraphy, and lithogeochemistry of an Archean volcanic arc: evolution from plume-related volcanism to arc rifting of SE Abitibi greenstone belt, Val-d'Or, Canada; Precambrian Research, v. 115, p. 223–260.
- Thurston, P.C., Ayer, J.A., Goutier, J. and Hamilton, M.A. 2008. Depositional gaps in the Abitibi greenstone belt stratigraphy: a key to exploration for syngenetic mineralization; Economic Geology, v. 103, p. 1097–1134.
- Wilkinson, L., Cruden, A.R. and Krogh, T.E. 1999. Timing and kinematics of post-Timiskaming deformation within the Larder Lake-Cadillac deformation zone, southwest Abitibi greenstone belt, Ontario, Canada; Canadian Journal of Earth Sciences, v. 36, p. 627–647.
- Wong, L., Davis, D.W., Krogh, T.E. and Robert, F. 1991. U-Pb zircon and rutile chronology of Archean greenstone formation and gold mineralization in the Val-d'Or region, Quebec; Earth and Planetary Science Letters, v. 104, p. 325–336.

Zweng, P.L., Mortensen, J.K. and Dalrymple, G.B. 1993. Thermochronology of the Camflo gold deposit, Malartic, Quebec: implications for magmatic underplating and the formation of gold-bearing quartz veins; *Economic Geology*, v. 88, p. 1700–1721.

FIGURES

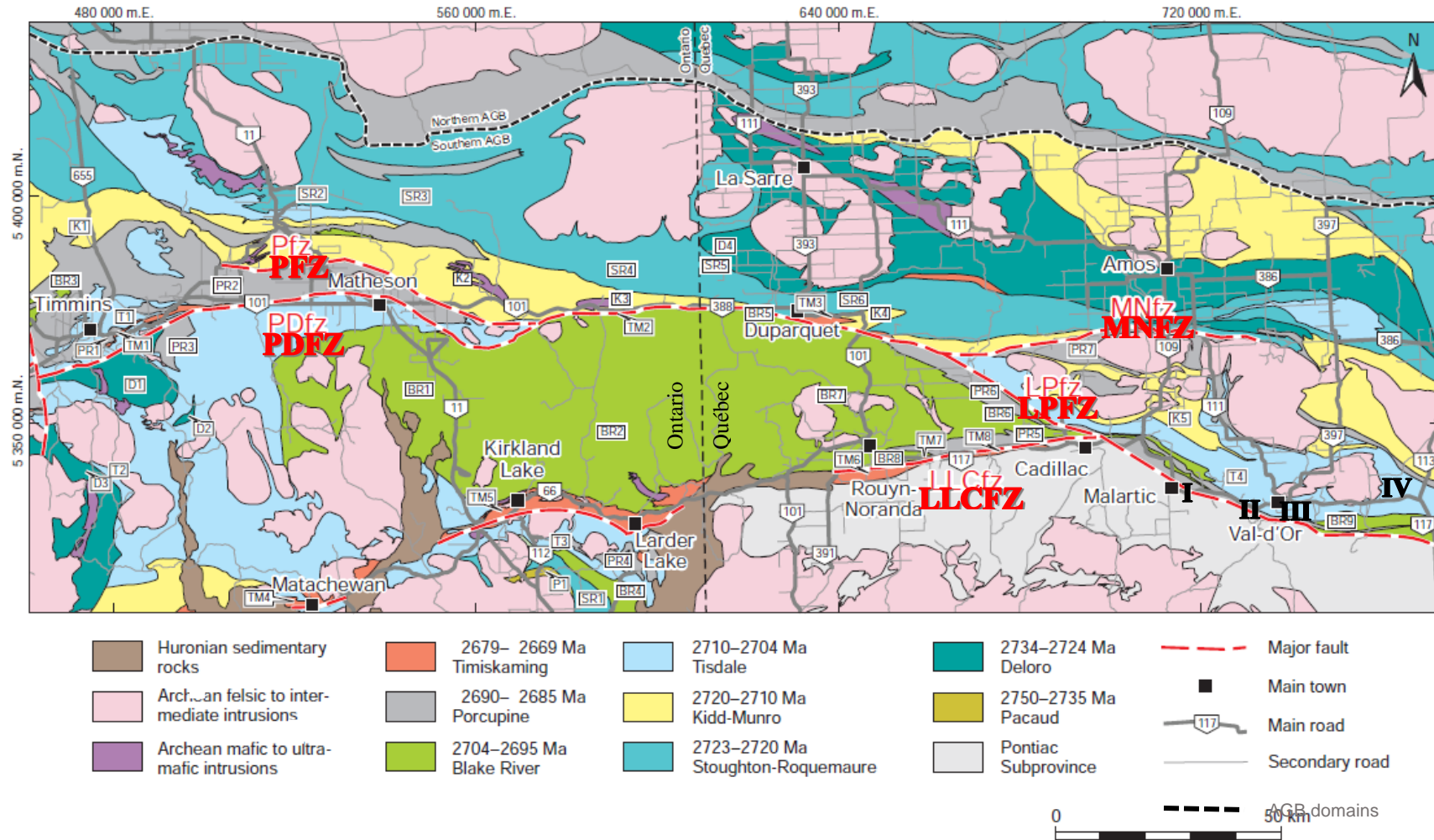


Figure 1. Geology of the southern Abitibi greenstone belt, showing samples collected in 2019 and the major chronostratigraphic assemblages that correspond to distinct volcanic and sedimentary periods during the formation of the southern Abitibi Subprovince. Deposits: Canadian Malartic (I); Goldex (II); Triangle (III); Pascalis Gold Trend (IV). Figure *modified from* Monecke et al. (2017). Abbreviations: AGB, Abitibi greenstone belt; LLCfZ, Larder Lake–Cadillac fault zone; LPfZ, La Pause fault zone; MNfZ, Manneville North fault zone; PDfZ, Porcupine–Destor fault zone; PfZ, Pipestone fault zone.

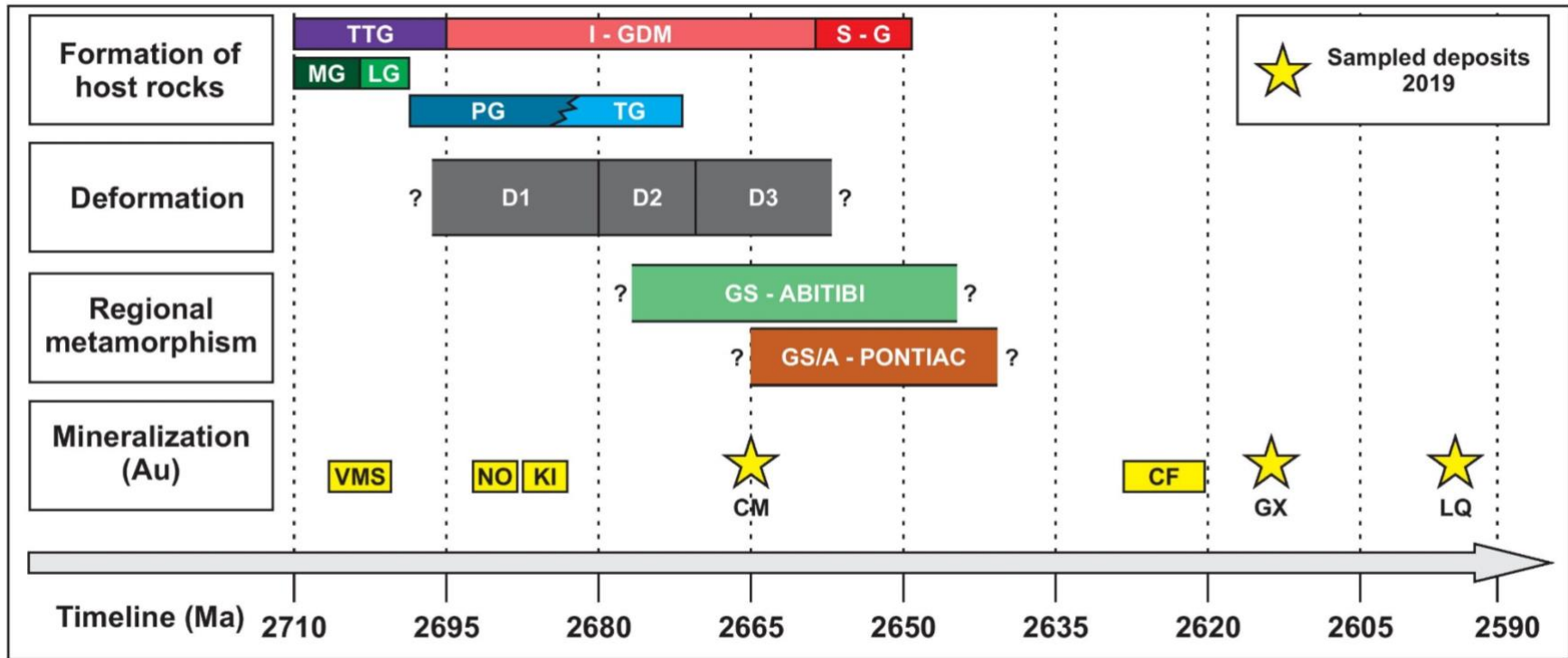


Figure 2. Simplified timeline showing major geological events that led to the formation of the Malartic–Val-d’Or area and associated gold mineralization: Camflo deposit (CF) Jemielita et al. (1990), Zweng et al. (1993); CM = Canadian Malartic, De Souza et al. (2017); D1-D2-D3 = deformation phases 1, 2, 3, Wilkinson et al. (1999), Bedeaux et al. (2017); GS = greenschist Abitibi, Powell et al. (1995); GS/A = greenschist/amphibolite Pontiac, Machado et al. (1991), Davis et al. (1994), Powell et al. (1995), Piette-Lauzière et al. (2019); GX = Goldex deposit, Geological Survey of Canada unpublished data; I-GDM = I-type granodiorite, diorite, monzonite, Beakhouse (2011); KI = Kiena deposit, Morasse et al. (1995); LG = Louvicourt group, Pilote et al. (1998a); LQ = Lamaque deposit, Wong et al. (1991); MG = Malartic group, Pilote et al. (1997), Scott et al. (2002); NO = Nolartic deposit, Couture et al. (1994); S-G = local S-type granite, Beakhouse (2011); TTG = tonalite, trondhjemite, granodiorite, Beakhouse (2011).

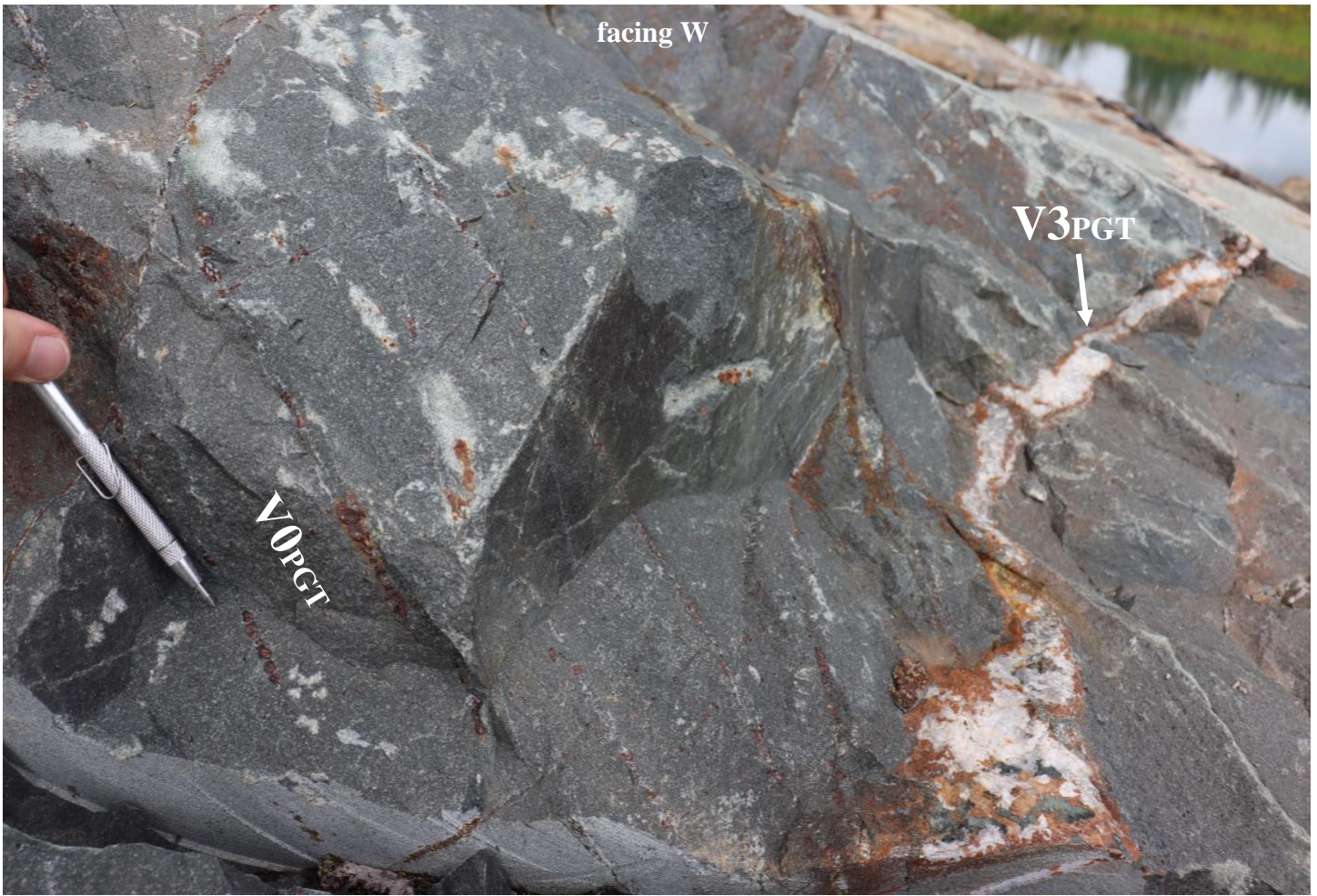


Figure 3. The main outcrop at the Pascalis Gold Trend deposit facing west. Thin, millimetre-sized sulphide-quartz veinlets ($V0_{PGT}$), visible as rusted sulphide minerals, are subparallel to north-dipping S_0 (and subparallel to tungsten pen) in a basalt unit with a late crosscutting quartz-tourmaline flat vein ($V3_{PGT}$) showing a rusty selvage due to weathering of tourmaline and sulphide minerals.